EFFECTS OF PREPARATION METHODS ON THE STRUCTURE AND MECHANICAL PROPERTIES OF WET CONDITIONED STARCH/MONTMORILLONITE NANOCOMPOSITE FILMS

Péter Müller[1,2], Éva Kapin[1,2], Erika Fekete[1,2*],

[1]Laboratory of Plastics and Rubber Technology, Department of Physical Chemistry and Materials Science, Budapest University of Technology and Economics, H-1521 Budapest, P.O. Box 91, Hungary

[2]Institute of Materials and Environmental Chemistry, Research Centre for Natural Sciences, Hungarian Academy of Sciences, H-1525 Budapest, P.O. Box 17, Hungary

*Corresponding author: Phone: +36-1-463-4335, Fax: +36-1-463-3474, Email: ebodine@mail.bme.hu

ABSTRACT

TPS/Na-montmorillonite nanocomposite films were prepared by solution and melt blending. Clay content changed between 0 and 25 wt% based on the amount of dry starch**.** Structure, tensile properties, and water content of wet conditioned films were determined as a function of clay content. Intercalated structure and V_H-type crystallinity of starch were found for all the nanocomposites independently of clay and plasticizer content or preparation method, but at larger than 10 wt% clay content nanocomposites prepared by melt intercalation contained aggregated particles as well. In spite of the incomplete exfoliation clay reinforces TPS considerably. Preparation method has a strong influence on mechanical properties of wet conditioned films. Mechanical properties of the conditioned samples prepared by solution homogenization are much better than those of nanocomposites prepared by melt blending. Water, which was either adsorbed or bonded in the composites in conditioning or solution mixing process, respectively, has different effect on mechanical properties.

KEYWORDS: TPS/montmorillonite nanocomposite, mechanical properties, wet conditioning, interfacial interactions

1. INTRODUCTION

Recently growing interest has been shown in the application of biopolymers as packaging materials in order to reduce the environmental pollution caused by plastic waste and to achieve sustainable development. Starch is considered as one of the most promising biopolymer because it is readily available, cheap and biodegradable. Starch is a semicrystalline polymer and it represents the major form of stored carbohydrate in plants. Starch is composed of repeating α-D glucopyranosyl units, a mixture of two substances, an essentially linear polysaccharide-amylose and a highly branched polysaccharide-amylopectin.

In amylose the repeating units are linked by α(1–4) linkages; the amylopectin has an α (1–4)-linked backbone and ca. 5 % of α (1–6)-linked branches (Averous, 2004; Avérous & Pollet, 2012; Hayashi, Kinoshita & Miyake, 1981; Zobel, 1988). The relative amounts of amylose and amylopectin depend upon the botanical source. Corn starch granules typically contain approximately 70 % amylopectin and 30% amylose (Lambert & Poncelet, 1997). The properties of starch depend strongly on the ratio of these two components. One of the major problems with granular starch is its limited processability, which can be improved by the use of plasticizers, i.e. thermoplastic starch (TPS). TPS can be obtained by the destruction of the starch granules in the presence of plasticizers under specific conditions. Polyols such as glycerol, glycols as well as water are the most widely used plasticizers (Averous, 2004; Avérous & Pollet, 2012; Chivrac, Pollet & Averous, 2009). The main disadvantages of TPS are its pronounced hydrophilic character and the inadequate mechanical properties. The inferior properties of TPS can be improved by the incorporation of other materials (natural fibers, nanoclays, or other biodegradable polymers) (Averous, 2004; Averous & Boquillon, 2004; Averous & Fringant, 2001; Averous, Fringant & Moro, 2001a, b; Chivrac, Pollet & Averous, 2009; Mitrus, 2010; Schwach & Averous, 2004; Vroman & Tighzert, 2009; Yixiang, Junjie & Milford, 2007).

Polymer/clay nanocomposites are assumed to exhibit improved barrier, thermal and mechanical properties comparing with traditional composites. Recently several attempts were reported in the literature for the preparation of TPS nanocomposites. In most cases TPS/montmorillonite nanocomposite films were prepared by melt blending (in internal batch mixer or in a twin screw extruder) (Avella, De Vlieger, Errico, Fischer, Vacca & Volpe, 2005; Chen & Evans, 2005; Chiou, Wood, Yee, Imam, Glenn & Orts, 2007; Chivrac, Pollet & Averous, 2009; Chivrac, Pollet, Dole & Averous, 2010; Dean, Yu & Wu, 2007; Huang, Yu & Ma, 2004; Magalhaes & Andrade, 2009; Muller, Laurindo & Yamashita, 2012; Ray &

Bousmina, 2005; Tang, Alavi & Herald, 2008) or solution mixing (film casting) (Chaudhary & Liu, 2013; Chivrac, Pollet & Averous, 2009; Cyras, Manfredi, Ton-That & Vazquez, 2008; Kampeerapappun, Aht-Ong, Pentrakoon & Srikulkit, 2007; Kelnar, Kapralkova, Brozova, Hromadkova & Kotek, 2013; Majdzadeh-Ardakani, Navarchian & Sadeghi, 2010; Masclaux, Gouanve & Espuche, 2010; Pandey & Singh, 2005; Ray & Bousmina, 2005; Schlemmer, Angelica & Sales, 2010). The results clearly demonstrated that the incorporation of organophilic montmorillonite with apolar character led to the formation of conventional microcomposites, while due to the polar nature of both starch and Na-montmorillonite **(**NaMMT) the application of NaMMT results in an intercalated/exfoliated structure of TPS nanocomposites (Chivrac, Pollet & Averous, 2009; Ray & Bousmina, 2005). Large extent of exfoliation was achieved using only water or less than 10 wt % glycerol as plasticizer (Chivrac, Pollet & Averous, 2009; Dean, Yu & Wu, 2007; Tang, Alavi & Herald, 2008). Several studies proved that the use of glycerol contents larger than 10 wt% led to the formation of intercalated structures with interlayer basal spacing (d001) increasing from 1.2 to 1.8 nm (Chiou, Wood, Yee, Imam, Glenn & Orts, 2007; Chivrac, Pollet & Averous, 2009; Pandey & Singh, 2005). It is difficult to verify whether the starch or the glycerol molecules intercalate between the clay layers, because both have a tendency to penetrate into the silicate layers, but penetration of glycerol is favored owing to its smaller molecular size (Aouada, Mattoso & Longo, 2011; Chaudhary & Liu, 2013). Several investigations confirm the strong influence of the polyol plasticizer on the exfoliation process and thus on the resulting morphology. This effect is likely related to the hydrogen bonds established between glycerol and MMT platelets, which could decrease the attractive forces between starch and clay (Chiou, Wood, Yee, Imam, Glenn & Orts, 2007; Chivrac, Pollet & Averous, 2009; Pandey & Singh, 2005). Exfoliated/intercalated morphology is found to be dependent also on NaMMT content. Exfoliation is the predominant mechanism of clay dispersion at small filler content

(Schlemmer, Angelica & Sales, 2010), while increasing the clay content above 5 wt.% favours the formation of intercalated structure.

In spite of incomplete exfoliation the TPS/NaMMT nanocomposites have improved properties compared to TPS. Its properties strongly depend on the type of the starch and the montmorillonite used, as well as on the amount of MMT and glycerol. Papers published so far indicate that larger extent of exfoliation results in better properties (Aouada, Mattoso & Longo, 2011; Chen & Evans, 2005; Chivrac, Pollet & Averous, 2009; Dean, Yu & Wu, 2007; Majdzadeh-Ardakani, Navarchian & Sadeghi, 2010; Muller, Laurindo & Yamashita, 2012; Schlemmer, Angelica & Sales, 2010; Tang, Alavi & Herald, 2008). Besides their barrier properties packaging materials should possess also proper mechanical characteristics. Although several papers discuss the stiffness, strength and deformability of TPS nanocomposite films (Aouada, Mattoso & Longo, 2011; Avella, De Vlieger, Errico, Fischer, Vacca & Volpe, 2005; Chivrac, Pollet, Dole & Averous, 2010; Chung, Ansari, Estevez, Hayrapetyan, Giannelis & Lai, 2010; Cyras, Manfredi, Ton-That & Vazquez, 2008; Dean, Yu & Wu, 2007; Huang, Yu & Ma, 2004; Majdzadeh-Ardakani, Navarchian & Sadeghi, 2010; Muller, Laurindo & Yamashita, 2012; Schlemmer, Angelica & Sales, 2010; Tang, Alavi & Herald, 2008), only a limited number of papers reports systematic experiments carried out as a function of filler content in a wide composition range (Aouada, Mattoso & Longo, 2011; Chen & Evans, 2005; Huang, Yu & Ma, 2004; Majdzadeh-Ardakani, Navarchian & Sadeghi, 2010), and often very poor mechanical properties are published compared to commodity polymers. Since packaging materials are not usually applied under dry conditions, the mechanical properties of the dry TPS/clay composites investigated generally are not relevant, because it is well known that humidity can strongly influence the strength and the stiffness of TPS nanocomposite films. In spite of this effect, relatively few papers have been published on TPS composites studied under ambient conditions (RH = 30-60 %) (Aouada, Mattoso &

Longo, 2011; Chung, Ansari, Estevez, Hayrapetyan, Giannelis & Lai, 2010; Huang, Yu & Ma, 2004). Furthermore the effect of processing technology on the properties of TPS nanocomposites of the same composition has not yet been thoroughly elucidated. Although (Aouada, Mattoso & Longo, 2011, 2013) prepared TPS nanocomposites by the combination of the intercalation from solution and melt-processing preparation methods and they found that the applied method resulted in intercalated/exfoliated structure and good thermal, mechanical properties as well as decreased hydrophobicity and water absorption, indeed, the measured mechanical properties were very poor and the different effect of the individual processes on the morphology and properties of TPS nanonocomposites was not investigated at all.

As a consequence, the goal of our work was to prepare TPS/NaMMT nanocomposite films with different glycerol and clay content using a melt blending as well as a solution mixing procedure and to determine the structure and properties of dry and wet (conditioned) films in a wide composition range. Considerable attention is paid also to interactions developing among the components.

2. EXPERIMENTAL

High quality corn starch produced in Hungary (Hungrana Ltd.) was used in the experiments. Glycerol was purchased from Aldrich, Hungary. Sodium montmorillonite (Cloisite Na+) with a cation exchange capacity (CEC) of 92.6 meq/100 g clay was supplied by Southern Clay Products ((Rockwood Additives Ltd.).

2.1. Preparation of plasticized starch/montmorillonite nanocomposite films

TPS nacomposite films were prepared by solution and melt blending. Solution mixing was carried out in the following way: Native starch was dispersed in the excess amount of

152 distilled water containing 30 and 40 wt % of glycerol. Then the suspension was continuously
153 stirred at 80 °C for 30 min to gelatinize the corn starch granules. The starch concentration of
154 the solution was 4.5 wt %. Sodium montmorillonite (NaMMT) was dispersed in distilled
155 water at concentration of 0.8 wt % by sonication for 30 min at room temperature. The clay
156 dispersion was added to the aqueous gelatinized starch and the mixture was stirred for another
157 30 min at 90 °C. Films were obtained by casting the hot suspension into Petri dishes covered
158 by a Teflon sheet and dried in an oven at 40 °C for 24 hours. Clay content changed between 0
159 and 25 wt% based on the amount of dry starch. Thickness of the films was 0.10 ± 0.02 mm.
160 Before the tests the films were stored at 23 °C and 52 % RH until constant weight was
161 reached. Nanocomposite films were also prepared by melt intercalation. During the process
162 the dry starch was premixed with glycerol (40 wt %) and montmorillonite in a Petri dish and
163 the mixtures were introduced into an internal mixer (Brabender W50 EH) and homogenized at
164 150 °C for 10 min. 0.10 mm ± 0.02 mm thick plates were compression molded from the melt
165 at 150 °C and 5 min. One part of the films prepared by melt mixing was stored under dry
166 conditions, while the other part was stored at 23 °C and 52 % RH until further study. Table 1
167 contains the list of nanocomposite films, their compositions and the methods used for their
168 preparation.
169
170 **2.2. Characterization**
171 The crystalline structure of TPS and the gallery structure of the filler were studied by
172 X-ray diffraction (XRD) using a Philips PW1830/PW1050 equipment with CuKα radiation at
173 40 kV and 35 mA. Samples were scanned in the diffraction angle range of 2–35° in 0.1° steps.
174 Diffractograms were recorded on powders (montmorillonite and starch) or films using a
175 multipurpose sample stage. The basal spacing of the silicate layers was calculated using the
176 Bragg's equation. The extent of crystallinity of starch was estimated dividing the crystalline

177 area by the total (crystalline + amorphous) area (Liu, Yu, Simon, Zhang, Dean & Chen,
178 2009).

179 The morphology of the samples was examined by scanning electron microscopy
180 (SEM) using a Jeol JSM 6380 apparatus. The micrographs were taken from surfaces created
181 by cutting with an ultramicrotome. The light transmission of the films was determined using
182 an UV-VIS spectrometer (Unicam W500) at various wavelengths. Only results obtained at
183 700 nm are reported here.

184 The equilibrium water content of the conditioned (at 23 °C at 52 % RH) film samples
185 was determined by thermogravimetric analysis (TGA). Thermogravimetric analysis (TGA)
186 was carried out in a Perkin Elmer TGA 6 equipment from 35 to 700 °C, at a heating rate of 10
187 °C/min, under nitrogen flow. The total weight loss up to 160 °C was identified as the water
188 content of the samples.

189 The tensile properties of the samples were measured using an Instron 5566 apparatus.
190 Young's modulus was determined at 0.5 mm/min while ultimate properties at a cross-head
191 speed of 5 mm/min. All characteristics were derived from five parallel measurements.

192 Properties of TPS nanocomposites were investigated as a function of volume fraction
193 of clay. In order to calculate the volume fraction of the filler we estimated the density of
194 nanocomposites from the compositions (NaMMT, starch, glycerol and water content)
195 assuming the additivity of densities of the components.

196

197 3. RESULTS AND DISCUSSION

198 The TPS nanocomposite films prepared by solution mixing or melt intercalation were
199 more or less transparent and showed homogeneous appearance without breaks, fractures,
200 insoluble particles or bubbles (Fig. 1). The films with smaller plasticizer content (water and

glycerol) appeared to be stiffer and more brittle than films containing more plasticizer. Cast films were white, while films prepared by compression molding showed brown color.

3.1. Structure

Crystallinity

Fig. 2a shows the XRD patterns obtained for the conditioned TPS (S30-0, S40-0 and M40-0) films prepared by different methods together with the XRD trace of the native starch. The amylopectin side chains of native starch can crystallize in three crystalline forms, namely, the A-type for cereal starches, the B-type for tuberous and amylose rich starch and the C-type which has a structure between those of the A- and B-types (vanSoest, Hulleman, deWit & Vliegenthart, 1996). These structures are completely or partially destroyed during processing resulting in an amorphous matrix. According to (vanSoest & Vliegenthart, 1997) two types of crystallinity can be distinguished in thermoplastic starch after processing: residual crystallinity and process-induced crystallinity. The residual crystallinity is caused by incomplete melting or solution of starch during processing and can be A-, B- or C-type, as occurs in native starches. The induced crystallinity is associated with the crystallization of amylose and identified as V_H-, V_A- or E_H-types.

It is well known that native corn starch crystallizes in the A-form and the characteristic diffraction peaks with strong reflections at 2θ angles of about 15° and 23° and an unresolved doublet at 17°and 18° can be easily identified in the XRD pattern of native starch in Fig. 2a indeed. The absence of these peaks in the XRD patterns of the cast TPS films clearly proves that the original crystalline structure was completely destroyed during the solution mixing process. Some minimal residual A-type crystallinity may be assumed in the TPS film prepared by melt process. The characteristic peaks at 2θ = 12.9°, 17.3°, 19.7° and 22.2° indicate the formation of the V_H-type structure in all films. V_H-type crystallinity is typical for

TPS samples in which the water content is larger than 10 wt% (Mitrus, 2010; vanSoest, Hulleman, deWit & Vliegenthart, 1996). The extent of starch crystallinity was also calculated for all TPS nanocomposites and the results are presented in Fig. 2b. From Fig. 2b it is obvious that nanocomposites containing 40 wt % glycerol have somewhat larger crystallinity than samples with 30 wt % glycerol content which is probably caused by the larger mobility of starch chains in TPS composites containing more plasticizer. Although the results indicate that the crystallinity of the matrix polymer increases with clay content, the overlapping of the characteristic peak of the clay at $2\theta = 20.05°$ (Zahedsheijani, Faezipour, Tarmian, Layeghi & Yousefi, 2012) and that of the starch at $2\theta = 19.7°$ must be considered here.

Dispersion of NaMMT in the TPS matrix

The 2θ range between 2° and 10° was analyzed in order to obtain information about the dispersion of the nanoclay in the TPS nanocomposites. Fig. 3a shows the XRD patterns of Cloisite-Na+, TPS (S30-0), and TPS–cloisite-Na+ nanocomposites (S30) prepared by solution mixing at different NaMMT contents. Starch does not have any characteristic reflection in the studied range while NaMMT exhibits a single 001 diffraction peak at around 7.3°. In the composite films the 001 diffraction peak of the NaMMT (1.21 nm) shifts to smaller angles (5.2° ± 0.2°) corresponding to an interlayer basal spacing (d001) of 1.69 ± 0.06 nm independently of clay content. Similar results were obtained also for the S40 and M40 samples. These results indicate that either the glycerol or the polymer chains or both entered into the silicate layers forming intercalated starch/MMT nanocomposites, without reaching complete exfoliation. The similar size of glycerol and glucose units in starch makes it difficult to assess, on the basis of the change in the interlayer spacing, whether starch, glycerol or both entered into the galleries.

Figure 3b presents the dependence of the intensity of clay reflection on clay content for nanocomposite films prepared by different methods. Intensity increases almost linearly with filler content up to approximately 3.0 vol % (10 wt % related to dry starch) in all samples, which indicates that exfoliation does not take place during processing or always the same fraction of the silicate exfoliates independently of clay content. Although the scattering of measured intensities of the M40 samples (prepared by melt intercalation) is quite large we can conclude that above 3 vol % clay content the extent of exfoliation is smaller in these nanocomposites than in samples prepared by solution mixing.

Further information can be obtained about the structure of the composites from their light transmission. Composites containing particles that are smaller than the wavelength of incident light are transparent while larger ones or aggregates scatter light, make the material opaque. Published results indicate that the transparency of nanocomposites increases with increasing extent of exfoliation (Manias, Touny, Wu, Strawhecker, Lu & Chung, 2001; Pozsgay, Csapo, Szazdi & Pukanszky, 2004; Wan, Qiao, Zhang & Zhang, 2003). Fig. 4 shows the transparency of our composites as a function of clay content. The light transmission of PVC/NaMMT composites is also plotted as reference (Pozsgay, Csapo, Szazdi & Pukanszky, 2004). We cannot expect any exfoliation to occur in this latter case. According to Fig. 4 large differences can be observed in the light transmission of the investigated TPS nanocomposites prepared by different procedures. The transparency of nanocomposites prepared by solution mixing remains large in the entire composition range, while that of the samples prepared by melt intercalation decreases significantly. Attention should be paid here to the small transparency of the TPS film prepared by melt blending without NaMMT (M40-0). The small transparency as well as the brown color of this sample might be related to the degradation of starch during melt homogenization. NaMMT obviously does not exfoliate at all in nanocomposites prepared by melt blending, while we may assume some exfoliation to occur

in samples prepared by solution mixing. The significant difference in the composition dependence of the transparency of nanocomposites prepared by various techniques does not coincide with their similar gallery distances and scattering intensities determined from the XRD patterns of the samples. Obviously we must not overemphasize either the changes in gallery distance or transparency, but we can safely conclude that during the preparation of TPS composites interactions take place among all components. Complete exfoliation definitely does not take place under the conditions used in this study, but intercalation and limited delamination cannot be excluded completely.

The degree of dispersion of NaMMT in the TPS composites was also investigated with the help of SEM micrographs. SEM micrographs taken from the S40-10 and M40-10 composites are presented in Fig. 5. These samples were prepared by different methods, but with the same glycerol and filler content. Several large clay aggregates of around 10 μm in diameter were observed in the starch film produced by melt intercalation, while the dispersion of NaMMT was homogeneous in the cast films and only very small particles could be seen in these samples. Similar homogeneous clay distribution was observed in all nanocomposite films (S30 and S40 samples) prepared by film casting.

3.2. Moisture content of conditioned nanocomposite films

The large water sorption capacity of TPS is well-known and better resistance against water is claimed to be one of the advantages of TPS composites containing layered silicates (Averous, 2004; Chivrac, Pollet & Averous, 2009). Absorbed water acts as plasticizer, thus influencing composite characteristics, mainly mechanical properties. TGA measurements were carried out on the samples of the TPS nanocomposite films prepared by solution or melt mixing and conditioned at 23 ° and 52 % relative humidity in order to determine the exact composition. The results are presented in Fig. 6 and indicate small differences in water

content, the original water content of TPS decreases by 3-4 wt% as the filler content increases by 7-8 vol %. The comparison of the water sorption capacity of the various cast films shows that TPS nanocomposites containing 40 wt % glycerol can absorb more water than samples with 30 wt % plasticizer content because of the high hygroscopicity of glycerol. The comparison of the films prepared by unlike methods is difficult, since different interactions can be formed between starch and water depending on the method of preparation.

3.3 Mechanical properties

Stiffness, strength and deformability of conditioned cast films as well as the same properties of dry and conditioned films prepared by melt intercalation were determined to characterize the mechanical behavior of the composites. The modulus, tensile strength and elongation-at-break values of the investigated TPS nanocomposites are plotted against clay content in Fig. 7. The figures clearly show that the mechanical properties of the samples strongly depend on their plasticizer (water and glycerol) and clay content. The standard deviation of the measurements is relatively large even though the films showed homogeneous appearance. According to Fig. 7a stiffness increases from around 0.70 GPa up to approximately 2.6 GPa for S30 and dry M40 films and from 0.10 GPa up to 0.45 GPa for S40 TPS nanocomposites, i.e. clay reinforce starch strongly. The S40 and dry M40 samples have almost the same plasticizer content, i.e. 40 wt% glycerol for M40 and 30 wt % glycerol + around 10 wt % water for S30 samples, thus the similar modulus of M40 and S30 films containing the same filler amount means that the preparation method has limited effect on stiffness and water seems to have stronger plasticizing effect than glycerol. Preparation technique, plasticizer content and the type of plasticizer have influence tensile strength and deformability more than modulus. The largest tensile strengths and the smallest elongation-at-breaks were measured for dry M40 nanocomposites in the 0-6 vol % NaMMT range.

According to Fig. 7b, tensile strength increases from 11.0 MPa up to 20.3 MPa. Above 3-4 vol % clay content composite strength does not increase further, which indicates the influence of some structural effect probably the inhomogeneous distribution of the filler discussed above. Presumably the strong plasticizing effect of water results in the smaller strength and larger deformability of the conditioned S30 samples compared to the dry M40 composite. With larger glycerol content tensile strength is smaller and elongation-at-break is larger. The tensile strength of the S40 nanocomposites is smaller than that of the S30 samples and the change with increasing NaMMT content is small (only approximately 3 MPa from 2.1 MPa to 5.2 MPa). It is important to note, however, that the stiffness and strength of conditioned M40 films are very poor, the worst among all samples in spite of the comparable glycerol and water content of S40 and conditioned M40 TPS nanocomposites. Probably the water is differently bonded during solvent mixing and conditioning and has different effect on mechanical properties. We mentioned earlier that the small transparency and brown color of the M40 samples might be related to the degradation of starch occurring during melt homogenization. If this assumption is true, it can explain the poorer mechanical properties of the conditioned M40 samples.

3.4. TPS/clay interaction

Interfacial interactions considerably influence and occasionally determine the properties of all heterogeneous materials. They play an important role also in the studied TPS/clay composites. Reinforcement or the strength of interaction can be estimated from composition dependence of the tensile strength of composites. The use of a simple semi-empirical model developed earlier (Pukánszky 1990), allows us to calculate a parameter (B) which is proportional to the load carried by the dispersed component. The model takes the following form for tensile strength

$$\sigma_T = \sigma_{T0}\lambda^n \frac{1-\varphi}{1+2.5\varphi}\exp(B\varphi) \quad (1)$$

where λ is the relative elongation (L/L_0), σ_T and σ_{T0} are the true tensile strength ($\sigma_T = \sigma\lambda$) of the composite and the matrix respectively, n is a parameter taking into account strain hardening, φ is the volume fraction of the filler and B is related to its relative load-bearing capacity, i.e. to the extent of reinforcement, which, among other factors, depends also on interfacial interaction. We can write Eq. 1 in linear form

$$\ln \sigma_{Tred} = \ln \frac{\sigma_T(1+2.5\varphi)}{\lambda^n(1-\varphi)} = \ln \sigma_{T0} + B\varphi \quad (2)$$

and plotting the natural logarithm of the reduced tensile strength of the composite (σ_{Tred}) against filler content should result in a linear correlation, the slope of which is proportional to parameter B. In Fig. 8 reduced tensile strength of the composites is plotted against filler content in the form indicated by Eq. 2. Relatively good straight lines are obtained for the three selected cases; standard deviation account for the scatter. The slope of the lines gives *B*. The parameters of the model, i.e. *B* and the intersection of the line, which corresponds to the calculated strength of the matrix, σ_{T0}, are listed in Table 2. The goodness of the linear fit, i.e. determination coefficient, is also listed in the table, in column four.

The value of *B* ranges from 12.0 to 16.8 for the conditioned S30 and S40, as well as for the dry M40 nocomposites, and they are very large compared to usual particulate filled commodity polymers; *B* is often smaller than 1 for PP/$CaCO_3$ composites e.g. (Kiss, Fekete & Pukanszky, 2007; Pukanszky, 1990). Similar, but slightly smaller *B* parameters (9.6-12.0) were determined for TPS/wood composites earlier (Müller, Renner, Móczó, Fekete & Pukánszky, 2013). We could not calculate parameter *B* for the conditioned M40 nanocomposite samples, because their tensile strength practically does not change with increasing filler content. The strength of the unfilled conditioned M40 TPS film was very poor (1.0 MPa).

Three main factors influence the value of *B*: the size of the contact surface between the components, the strength of interaction and the tensile strength of the matrix (σ_0). The first may increase considerably as a result of exfoliation, while the second is determined by the character of interaction (secondary forces, covalent bonds). *B* is defined as

$$B = \left(1 + A_f \varphi_f \ell\right) \ln \frac{\sigma_i}{\sigma_0} \qquad (3)$$

where A_f and ρ_f are the specific surface area and density of the reinforcing component, ℓ the thickness of the interphase forming spontaneously in the composite, while σ_i and σ_0 is the strength of the interface and the matrix, respectively. We could see in Fig. 3b that the extent of exfoliation is similar in the three investigated TPS nanocomposites in the range of 0-3 vol % clay content. It has also been proven earlier that the properties of the matrix (σ_0) play an important role in the actual value of B (Müller, Renner, Móczó, Fekete & Pukánszky, 2013; Szazdi, Pozsgay & Pukanszky, 2007). The softer is the matrix, the larger is the reinforcing effect of filler. Comparing the *B* parameters determined for the S30 and S40 nanocomposites we can see that *B* calculated for the S30 composites is larger than the one for S40. This is rather surprising, since the tensile strength of the S40-0 TPS matrix is much smaller than that of the S30-0 sample. Assuming similar extent of exfoliation of the montmorillonite in the different nanocomposites we can conclude that somewhat stronger interfacial interaction forms between the starch and the clay in the S30 samples than in the S40 composites. The probable reason for the stronger interaction is the smaller amount of glycerol applied for plasticization. As described in the introductory part, competitive interactions develop among starch, glycerol and clay and several authors (Chiou, Wood, Yee, Imam, Glenn & Orts, 2007; Chivrac, Pollet & Averous, 2009; Pandey & Singh, 2005) pointed out that the presence of glycerol may hinder the interaction between starch and montmorillonite. The comparison of the *B* value of the M40 samples with those of the S30 and S40 nanocomposites is difficult

because of the different preparation techniques used and because of dissimilar plasticizer contents.

4. CONCLUSIONS

According to the results of X-ray diffraction analysis, scanning electron microscopy and light transmission measurements all nanocomposites possess intercalated structure, but at larger clay content (above 10 wt%) nanocomposites prepared by melt intercalation contained aggregated particles as well. V_H-type crystallinity was found in all nanocomposites, which is typical for TPS containing more than 10 wt% water. Somewhat larger crystallinity was observed in nanocomposites containing more plasticizer, which is probably due to the larger mobility of starch molecules in these composites. The applied clay content was much larger than the usual 1-5 wt %, and the results proved that these nanocomposites can offer good properties in spite of the lack of the complete exfoliation. Clay reinforces TPS considerably in nanocomposites prepared by solution homogenization. Similarly good mechanical properties were determined also on dry samples prepared by melt blending, but conditioning of these samples resulted in very poor stiffness and strength, the worst among all samples studied. We assume that water either adsorbed or bonded in the composites in conditioning or solution mixing processes, respectively, has different effect on mechanical properties. With the aid of a simple model we could prove the strong interaction between starch and montmorillonite and that the increase in glycerol content decreases the starch/clay interaction.

5. ACKNOWLEDGEMENTS

The financial support of the National Scientific Research Fund of Hungary (OTKA Grant No. K 67936 and K 108934) to the research on polymer nanocomposite films and functional polymers is highly appreciated.

6. REFERENCES

Aouada, F. A., Mattoso, L. H. C., & Longo, E. (2011). New strategies in the preparation of exfoliated thermoplastic starch-montmorillonite nanocomposites. *Industrial Crops and Products, 34*(3), 1502-1508.

Aouada, F. A., Mattoso, L. H. C., & Longo, E. (2013). Enhanced bulk and superficial hydrophobicities of starch-based bionanocomposites by addition of clay. *Industrial Crops and Products, 50*, 449-455.

Avella, M., De Vlieger, J. J., Errico, M. E., Fischer, S., Vacca, P., & Volpe, M. G. (2005). Biodegradable starch/clay nanocomposite films for food packaging applications. *Food Chemistry, 93*(3), 467-474.

Averous, L. (2004). Biodegradable multiphase systems based on plasticized starch: A review. *Journal of Macromolecular Science-Polymer Reviews, C44*(3), 231-274.

Averous, L., & Boquillon, N. (2004). Biocomposites based on plasticized starch: thermal and mechanical behaviours. *Carbohydrate Polymers, 56*(2), 111-122.

Averous, L., & Fringant, C. (2001). Association between plasticized starch and polyesters: Processing and performances of injected biodegradable systems. *Polymer Engineering and Science, 41*(5), 727-734.

Averous, L., Fringant, C., & Moro, L. (2001a). Plasticized starch-cellulose interactions in polysaccharide composites. *Polymer, 42*(15), 6565-6572.

Averous, L., Fringant, C., & Moro, L. (2001b). Starch-based biodegradable materials suitable for thermoforming packaging. *Starch-Starke, 53*(8), 368-371.

Avérous, L., & Pollet, E. (2012). Biodegradable Polymers. In L. Avérous & E. Pollet (Eds.). *Environmental Silicate Nano-Biocomposites* (pp. 13-39): Springer London.

Chaudhary, D., & Liu, H. H. (2013). Ultrasonic treatment and synthesis of sugar alcohol modified Na+-montmorillonite clay. *Ultrasonics Sonochemistry*, *20*(1), 63-68.

Chen, B. Q., & Evans, J. R. G. (2005). Thermoplastic starch-clay nanocomposites and their characteristics. *Carbohydrate Polymers, 61*(4), 455-463.

Chiou, B. S., Wood, D., Yee, E., Imam, S. H., Glenn, G. M., & Orts, W. J. (2007). Extruded starch-nanoclay nanocomposites: Effects of glycerol and nanoclay concentration. *Polymer Engineering and Science, 47*(11), 1898-1904.

Chivrac, F., Pollet, E., & Averous, L. (2009). Progress in nano-biocomposites based on polysaccharides and nanoclays. *Materials Science & Engineering R-Reports, 67*(1), 1-17.

Chivrac, F., Pollet, E., Dole, P., & Averous, L. (2010). Starch-based nano-biocomposites: Plasticizer impact on the montmorillonite exfoliation process. *Carbohydrate Polymers, 79*(4), 941-947.

Chung, Y. L., Ansari, S., Estevez, L., Hayrapetyan, S., Giannelis, E. P., & Lai, H. M. (2010). Preparation and properties of biodegradable starch-clay nanocomposites. *Carbohydrate Polymers, 79*(2), 391-396.

Cyras, V. P., Manfredi, L. B., Ton-That, M. T., & Vazquez, A. (2008). Physical and mechanical properties of thermoplastic starch/montmorillonite nanocomposite films. *Carbohydrate Polymers, 73*(1), 55-63.

Dean, K., Yu, L., & Wu, D. Y. (2007). Preparation and characterization of melt-extruded thermoplastic starch/clay nanocomposites. *Composites Science and Technology, 67*(3-4), 413-421.

Hayashi, A., Kinoshita, K., & Miyake, Y. (1981). The conformation of amylose in solution.1. *Polymer Journal, 13*(6), 537-541.

Huang, M. F., Yu, J. G., & Ma, X. F. (2004). Studies on the properties of Montmorillonite-reinforced thermoplastic starch composites. *Polymer, 45*(20), 7017-7023.

Kampeerapappun, P., Aht-Ong, D., Pentrakoon, D., & Srikulkit, K. (2007). Preparation of cassava starch/montmorillonite composite film. *Carbohydrate Polymers, 67*(2), 155-163.

Kelnar, I., Kapralkova, L., Brozova, L., Hromadkova, J., & Kotek, J. (2013). Effect of chitosan on the behaviour of the wheat B-starch nanocomposite. *Industrial Crops and Products, 46*, 186-190.

Kiss, A., Fekete, E., & Pukanszky, B. (2007). Aggregation of CaCO3 particles in PP composites: Effect of surface coating. *Composites Science and Technology, 67*(7-8), 1574-1583.

Lambert, J. F., & Poncelet, G. (1997). Acidity in pillared clays: Origin and catalytic manifestations. *Topics in Catalysis, 4*(1-2), 43-56.

Liu, H. S., Yu, L., Simon, G., Zhang, X. Q., Dean, K., & Chen, L. (2009). Effect of annealing and pressure on microstructure of cornstarches with different amylose/amylopectin ratios. *Carbohydrate Research, 344*(3), 350-354.

Magalhaes, N. F., & Andrade, C. T. (2009). Thermoplastic corn starch/clay hybrids: Effect of clay type and content on physical properties. *Carbohydrate Polymers, 75*(4), 712-718.

Majdzadeh-Ardakani, K., Navarchian, A. H., & Sadeghi, F. (2010). Optimization of mechanical properties of thermoplastic starch/clay nanocomposites. *Carbohydrate Polymers, 79*(3), 547-554.

Manias, E., Touny, A., Wu, L., Strawhecker, K., Lu, B., & Chung, T. C. (2001). Polypropylene/Montmorillonite nanocomposites. Review of the synthetic routes and materials properties. *Chemistry of Materials, 13*(10), 3516-3523.

Masclaux, C., Gouanve, F., & Espuche, E. (2010). Experimental and modelling studies of transport in starch nanocomposite films as affected by relative humidity. *Journal of Membrane Science, 363*(1-2), 221-231.

Mitrus, M. (2010). TPS and Its Nature. *Thermoplastic Starch* (pp. 77-104): Wiley-VCH Verlag GmbH & Co. KGaA.

Muller, C. M. O., Laurindo, J. B., & Yamashita, F. (2012). Composites of thermoplastic starch and nanoclays produced by extrusion and thermopressing. *Carbohydrate Polymers, 89*(2), 504-510.

Müller, P., Renner, K., Móczó, J., Fekete, E., & Pukánszky, B. (2014). Thermoplastic starch/wood composites: Interfacial interactions and functional properties. *Carbohydrate Polymers, 102*, 821-829.

Pandey, J. K., & Singh, R. P. (2005). Green nanocomposites from renewable resources: Effect of plasticizer on the structure and material properties of clay-filled starch. *Starch-Starke, 57*(1), 8-15.

Pozsgay, A., Csapo, I., Szazdi, L., & Pukanszky, B. (2004). Preparation, structure, and properties of PVC/montmorillonite nanocomposites. *Materials Research Innovations, 8*(3), 138-139.

Pukanszky, B. (1990). Influence of interface interaction on the ultimate tensile properties of polymer composites. *Composites, 21*(3), 255-262.

Ray, S. S., & Bousmina, M. (2005). Biodegradable polymers and their layered silicate nanocomposites: In greening the 21st century materials world. *Progress in Materials Science, 50*(8), 962-1079.

Schlemmer, D., Angelica, R. S., & Sales, M. J. A. (2010). Morphological and thermomechanical characterization of thermoplastic starch/montmorillonite nanocomposites. *Composite Structures, 92*(9), 2066-2070.

Schwach, E., & Averous, L. (2004). Starch-based biodegradable blends: morphology and interface properties. *Polymer International, 53*(12), 2115-2124.

Szazdi, L., Pozsgay, A., & Pukanszky, B. (2007). Factors and processes influencing the reinforcing effect of layered silicates in polymer nanocomposites. *European Polymer Journal, 43*(2), 345-359.

Tang, X. Z., Alavi, S., & Herald, T. J. (2008). Effects of plasticizers on the structure and properties of starch-clay nanocomposite films. *Carbohydrate Polymers, 74*(3), 552-558.

vanSoest, J. J. G., Hulleman, S. H. D., deWit, D., & Vliegenthart, J. F. G. (1996). Crystallinity in starch bioplastics. *Industrial Crops and Products, 5*(1), 11-22.

vanSoest, J. J. G., & Vliegenthart, J. F. G. (1997). Crystallinity in starch plastics: Consequences for material properties. *Trends in Biotechnology, 15*(6), 208-213.

Vroman, I., & Tighzert, L. (2009). Biodegradable Polymers. *Materials, 2*(2), 307-344.

Wan, C. Y., Qiao, X. Y., Zhang, Y., & Zhang, Y. X. (2003). Effect of different clay treatment on morphology and mechanical properties of PVC-clay nanocomposites. *Polymer Testing, 22*(4), 453-461.

Yixiang, X., Junjie, G., & Milford, A. H. (2007). Starch-Based Biodegradable Packaging. *Encyclopedia of Agricultural, Food, and Biological Engineering* (Vol. null, pp. 1-4): Taylor & Francis.

Zahedsheijani, R., Faezipour, M., Tarmian, A., Layeghi, M., & Yousefi, H. (2012). The effect of Na+ montmorillonite (NaMMT) nanoclay on thermal properties of medium density fiberboard (MDF). *European Journal of Wood and Wood Products, 70*(5), 565-571

Zobel, H. F. (1988). Molecules to granules – a comprehensive starch review. *Starch-Starke, 40*(2), 44-50.

545 Table 1. Preparation method and composition as well as designation of TPS nanocomposites

Sample	Method	Glycerol content (g/100g starch)	Clay content	
			g/100 g starch	(vol %)
S30	Solution	30	0 - 25	0 - 8
S40	Solution	40	0 - 25	0 - 7
M40	Melt	40	0 - 25	0 - 7

546
547

548 Table 2. Calculated tensile strengths of TPS matrices, load-bearing capacities of clays and
549 the goodness of linear fits

Sample	σ_0 (MPa)	B	R^2
S30 nanocomposites	6.8	15.47	0.9612
S40 nanocomposites	2.2	11.97	0.9783
Dry M40 nanocomposites	10.8	16.80	0.9752

550

551

552 CAPTIONS

553

554 Fig. 1 Different appearence of TPS nanocomposites prepared by solution (left) and
555 melt blending (right)

556 Fig. 2 Crystalline structure of TPS/NaMMT nanocomposites: a) X-ray patterns of
557 starch and TPS samples prepared by different methods; b) Effect of clay
558 content on the crystallinity of TPS nanocomposites

559 Fig. 3 X-ray results: a) X-ray spectra of NaMMT, TPS and S30 nanocomposites; b)
560 Integrated intensity of the clay reflection plotted against clay content

561 Fig. 4 Effect of clay content on the transparency of different TPS/clay and PVC/clay
562 composites

563 Fig. 5 Scanning electron micrographs recorded on the cryo-cut surfaces of S40-10 (a)
564 and M40-10 (b) TPS/NaMMT nanocomposites

565 Fig. 6 Effect of filler and glycerol content as well as preparation technique on the
566 equilibrium water content of TPS nanocomposites

567 Fig. 7 Mechanical properties: effect of NaMMT content on the stiffness (a), strength
568 (b) and elongation-at-break (c) of TPS/NaMMT nanocomposites

569 Fig. 8 Tensile strength of TPS/NaMMT nanocomposites plotted against filler content
570 in the linear representation of Eq. (1)

571

572

573

574

575

576

Müller, Fig. 1

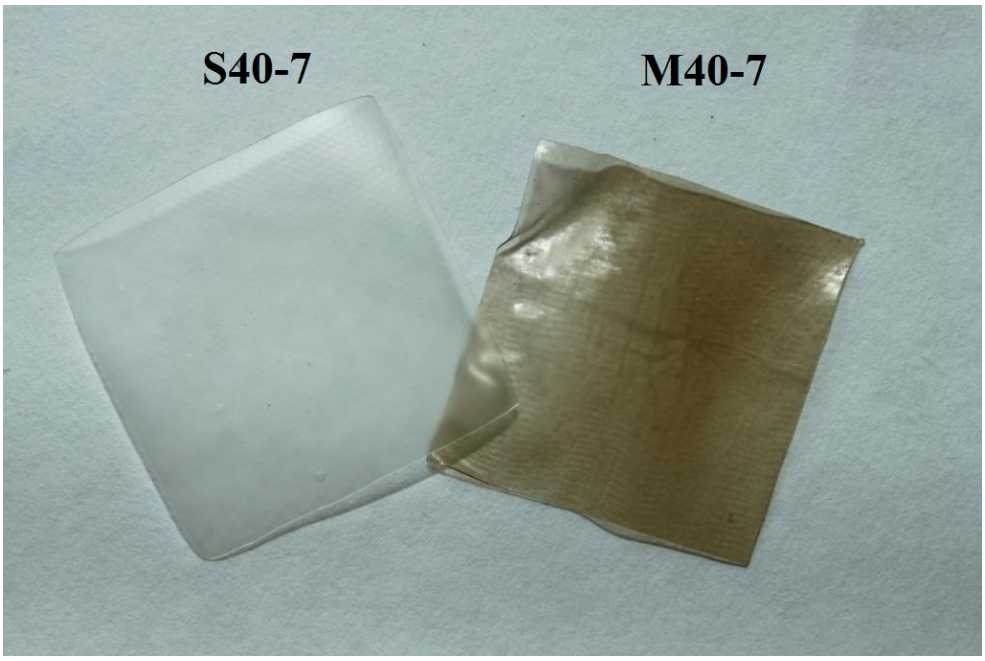

Fig. 1 Different appearence of TPS nanocomposites prepared by solution (left) and melt blending (right)

Müller, Fig. 2

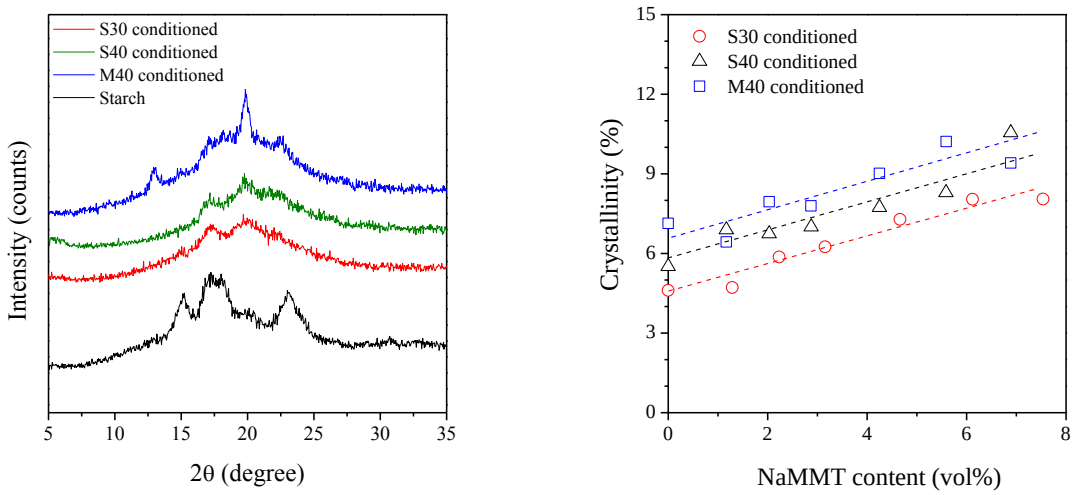

a) b)

Fig. 2 Crystalline structure of TPS/NaMMT nanocomposites: a) X-ray patterns of starch and TPS samples prepared by different methods; b) Effect of clay content on the crystallinity of TPS nanocomposites

Müller, Fig. 3

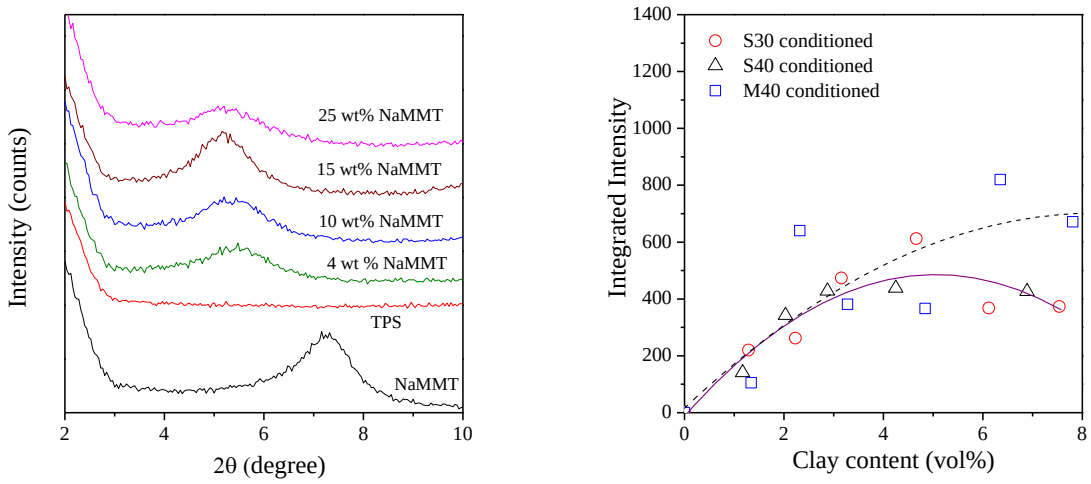

a) b)

Fig. 3 X-ray results: a) X-ray spectra of NaMMT, TPS and S30 nanocomposites; b) Integrated intensity of the clay reflection plotted against clay content

605 Müller, Fig. 4
606
607

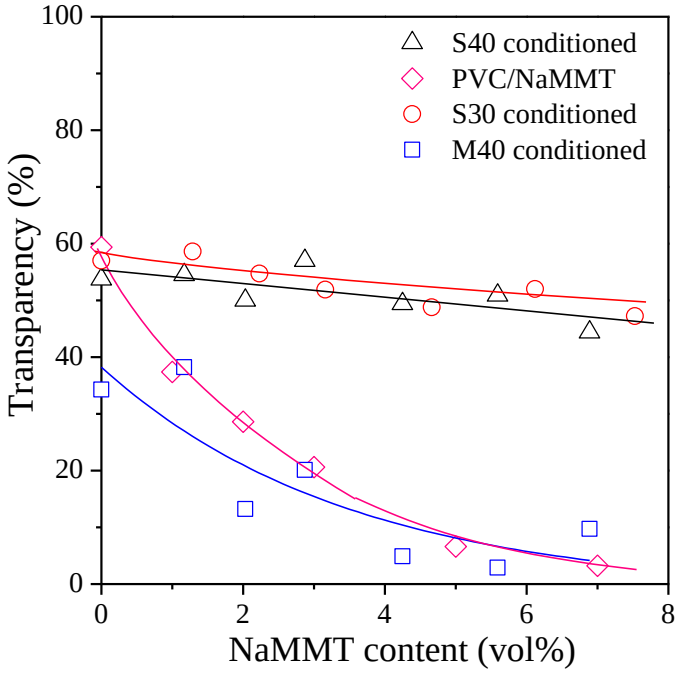

608
609 Fig. 4 Effect of clay content on the transparency of different TPS/clay and PVC/clay
610 composites

611
612

Müller, Fig. 5

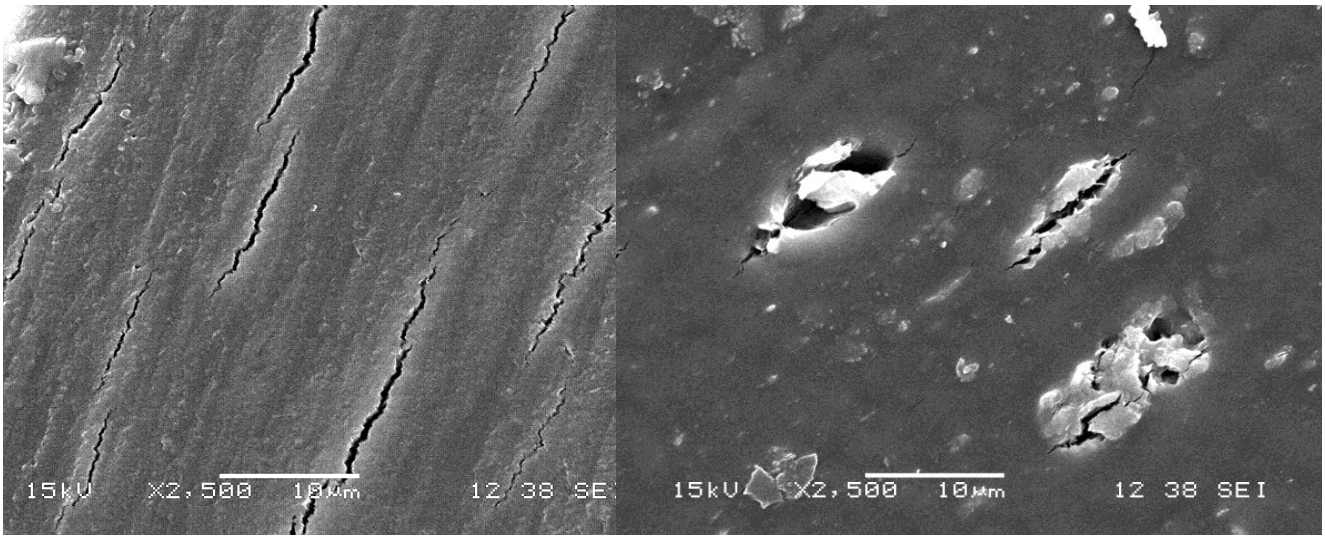

a) b)

Fig. 5 Scanning electron micrographs recorded on the cryo-cut surfaces of S40-10 (a) and M40-10 (b) TPS/NaMMT nanocomposites

Müller, Fig. 6

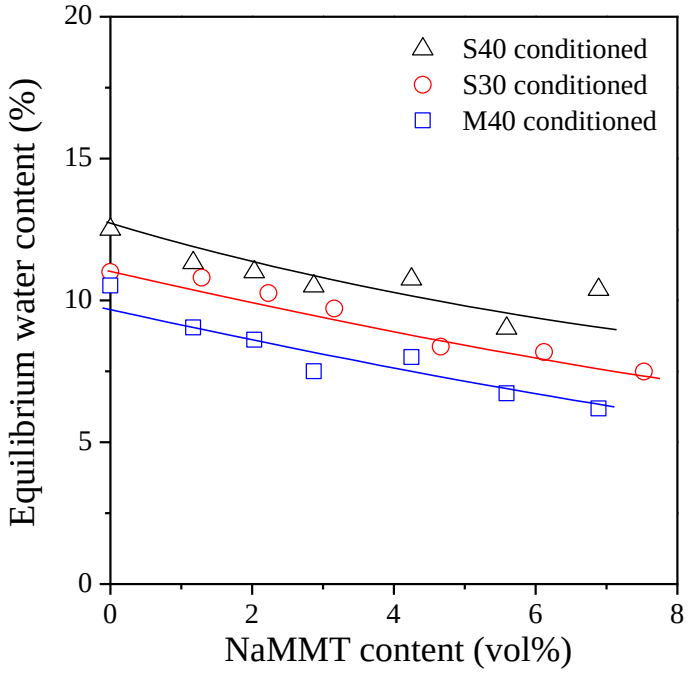

Fig. 6 Effect of filler and glycerol content as well as preparation technique on the equilibrium water content of TPS nanocomposites

629 Müller, Fig. 7

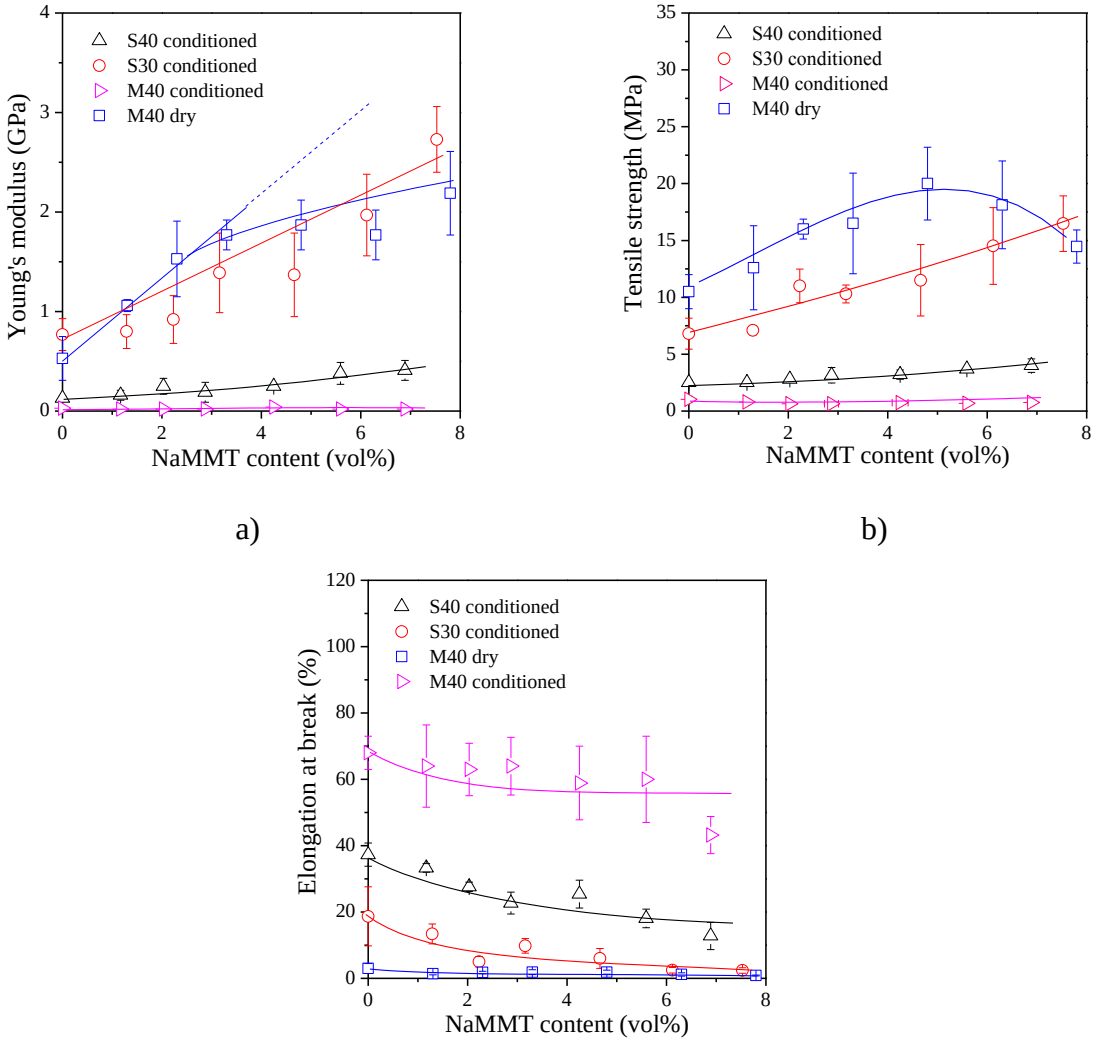

630
631

632 Fig. 7 Mechanical properties: effect of NaMMT content on the stiffness (a), strength

633 (b) and elongation-at-break (c) of TPS/NaMMT nanocomposites

634
635
636

637 Müller, Fig. 8
638
639

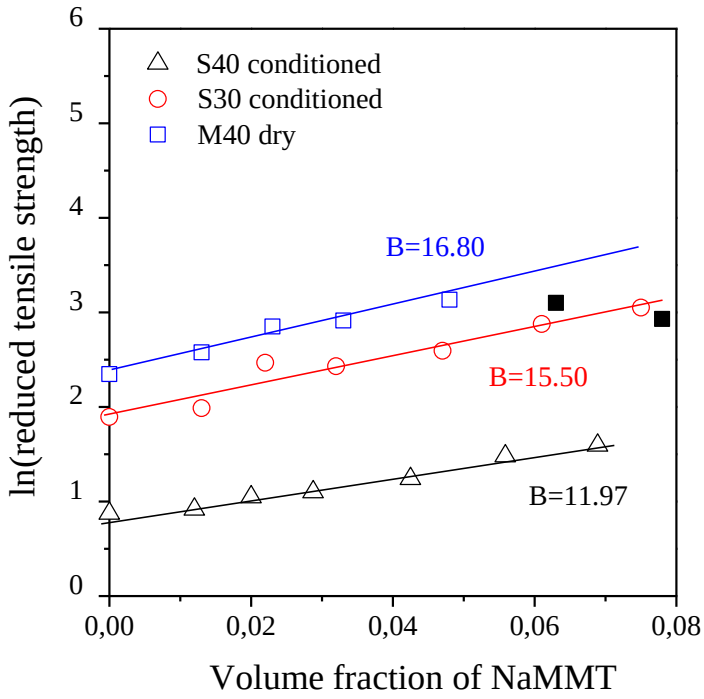

640
641
642 Fig. 8 Tensile strength of TPS/NaMMT nanocomposites plotted against filler content
643 in the linear representation of Eq. (1)
644
645